

# Energy-Efficient RIS-assisted Satellites for IoT Networks

Kürşat Tekbıyık, *Student Member, IEEE*, Güneş Karabulut Kurt, *Senior Member, IEEE*,  
Halim Yanikomeroglu, *Fellow, IEEE*

**Abstract**—The use of satellites to provide ubiquitous coverage and connectivity for the densely deployed Internet of Things (IoT) networks are expected to be a reality in the emerging 6G networks. Yet, the low battery capacity is of IoT nodes constitute a problem for the direct connectivity to satellites that are located up to 2000 km altitude. As an architectural novelty, in this paper we propose the use of reconfigurable intelligent surface (RIS) units to help with the path loss associated with high transmission distances. The use of RIS units through broadcasting and beamforming approaches are shown to provide a significant gain in terms of their signal transmission. These units can be placed on the reflectarrays that are already available on the satellites. It is shown that RIS-assisted satellites can provide up to  $10^5$  times higher downlink and uplink achievable rates for IoT networks.

**Index Terms**—Reconfigurable intelligent surfaces, LEO satellites, energy-efficient IoT networks.

## I. INTRODUCTION

Around 100 billion devices are expected to be connected in a massive ecosystem by vendors and business advisory companies, [1, 2]. Internet of Things (IoT) networks are expected to grow with approximately 20 percent compound annual growth rates [3]. By leveraging ubiquitous IoT networks, it is possible to enhance the efficiency in industries such as transportation, health, and maritime. Another prominent feature of massive IoT networks is to improve the quality of life. Although ubiquitous and massive IoT networks have tremendous development and appealing features for human life and industry, it is obviously foreseen that the backhauling for these ultra-massive networks require more attention to deal with the connection problem due to 4 billion people without an Internet connection [4]. To acquire wide coverage for the Internet, satellite recently gains more attention. Moreover, supporting IoT services with satellite networks is a prominent research topic for both academia and industry.

### A. Related Works

Recently, an architecture has been proposed for the use of geostationary orbit (GEO) satellites in narrowband-IoT applications [5, 6]. However, it should be noted that GEO satellites are exposed to very high path losses and very long delay due to their relatively long distance from the ground. To eliminate the drawback of GEO satellites, low-Earth orbit

(LEO) satellite constellations for IoT is introduced in [7, 8] because LEO satellite orbits are closer to the Earth than that of GEO satellites. Thus, LEO satellites require less transmission power to keep required signal-to-noise ratio (SNR) for proper communication. But., LEO constellations bring the drawbacks which are steerable antenna and tracking requirements due to motion with relatively high velocity. Obviously, these requirements are unlikely to meet such computational and hardware complexity for IoT devices with low-complexity hardware and low battery capacity. In order to remove the effects of these drawbacks from IoT devices, it is proposed to use reconfigurable intelligent surfaces (RISs) in LEO satellites in this study. RISs intelligently adjust the phase shifts of elements in order to maximize the received power [9]. The most appealing feature of RIS is that they comprise of passive circuit elements completely. Furthermore, complex processing or coding is not required by RISs. Moreover, its effectiveness is also demonstrated by experimental measurements in [10, 11].

LEO satellites do not require a serious hardware improvement, as RISs have a simple hardware structure consisting of passive circuit elements [12]. Moreover, the hardware complexity of IoT devices can be reduced as RISs allow signal processing to be performed in the transmission environment rather than on the devices [9]. Thus, battery-constrained IoT devices can operate for a longer duration. Furthermore, RISs are able to enable energy efficient wireless communication while keeping the quality of service (QoS) same [13]. As RIS units provide the energy efficiency and low hardware complexity for wireless communications, the use of RIS can be a game-changer for satellite-IoT systems. Furthermore, our previous work [12] demonstrates that error probability can be reduced in LEO inter-satellite links by utilizing RIS.

### B. Motivations

As the number of IoT applications increases, along with almost exponentially increasing number of devices, ubiquitous coverage requirement becomes more apparent. The emerging LEO satellite networks provide an appealing means for this connectivity requirement. With a high number of satellites in near Earth constellations, the likelihood of getting continuous service from a satellite is planned to be really high. Providing IoT services over LEO networks constitute a synergy that has been under investigation not only by the research community but also by the standardization organizations, such as 3GPP, and private companies, such as Sateliot. Especially with the 5G standards, following the 3GPP TR 36.763 [14], IoT

K. Tekbıyık and G.K. Kurt are with the Department of Electronics and Communications Engineering, Istanbul Technical University, Istanbul, Turkey, e-mails: {tekbiyik, gkurt}@itu.edu.tr

H. Yanikomeroglu is with the Department of Systems and Computer Engineering, Carleton University, Ottawa, Canada, e-mail: halim@sce.carleton.ca

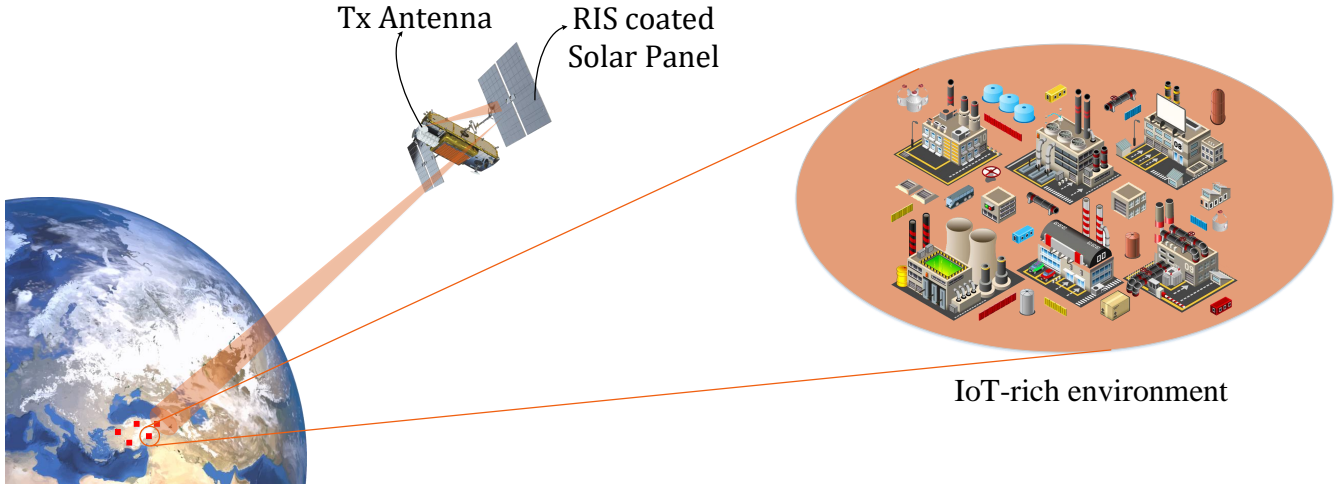


Fig. 1. It is possible to enhance the QoS for satellite-IoT systems by utilizing RIS. Therefore, the required power can be reduced for the same data rate and error probability.

deployments over satellites will be a reality in the near future, not only targeting rural areas that do not get sufficient coverage but also improving the capacity in highly populated dense deployments in mega-cities.

As the IoT devices have limited battery lives, any boost in the link budget will be useful in satellite networks. To address this issue in this paper we propose the use of receive RIS to improve received power levels. RIS units are composed of metasurfaces that are controlled in real time to adjust the reflection phases [9]. Their potential has already been apparent in the recent works including [13, 15]. In this paper, we propose the use of RIS located at your satellites that can be positioned jointly with a reflective array as illustrated in Fig. 1. After formulating the problem we quantify the possible transmit power gain for the target performance is detailed below.

### C. Contributions

Our contributions on the way to provide ubiquitous and dense connectivity demanded by 6G and beyond are summarized below:

- C1 A novel architecture is proposed for IoT networks based on the use of RIS units at the satellites. These are RIS units can be placed on the rectenna arrays.
- C2 We derive the SNR levels of LEO satellites to support IoT networks considering broadcasting and beamforming modes based on the transmission characteristics including the carrier frequency.
- C3 Through extensive numerical results, we quantification of the potential reduction for the transmit power well considering a realistic transmission model. Based on our analysis, we suggest design guidelines for future IoT networks that are served by LEO satellites.

### D. Outline

The rest of this paper is organized as follows. Section II introduces the associated free space path loss models for RIS-assisted broadcasting and RIS-assisted beamforming schemes

as well as the case without RIS. In Section III, the system model is described for RIS-assisted LEO satellites for IoT networks. Section IV presents extensive numerical results and observations for non-RIS satellites and RIS-assisted satellites with bot broadcasting and beamforming schemes. Open issues are discussed in Section V. Finally, the study is concluded in Section VI.

## II. PRELIMINARIES

We discuss the mathematical and physical preliminaries for RIS-assisted satellites for IoT networks and give the foundation information in this section. Firstly, we remind free space path loss for conventional satellite systems. Then, path loss modeling for RIS-assisted wireless communications is introduced. Here, the notation is given for downlink; however, it can be generalized for uplink case in a straightforward manner.

### A. Free Space Path Loss

The ratio of the received and transmitted powers in a link between two isotropic antennas can be given by free space path loss, which is defined as follows:

$$L_{FS} = (4\pi d/\lambda)^\alpha, \quad (1)$$

where  $\alpha$  and  $\lambda$  denote the path loss exponent and wavelength, respectively.  $d$  is the distance between satellite and ground station which can be obtained as:

$$d = -r_e \sin(\varphi) + \sqrt{r_e^2 \sin^2(\varphi) + h_{sat}^2 + 2r_e h_{sat}}, \quad (2)$$

where  $r_e$ ,  $h_{sat}$ , and  $\varphi$  are the radius of Earth, the altitude of satellite, and the elevation angle between the ground station and satellite, respectively. The path loss is proportional to  $d^\alpha$ ; therefore, the elevation angle has an important role on the path loss.

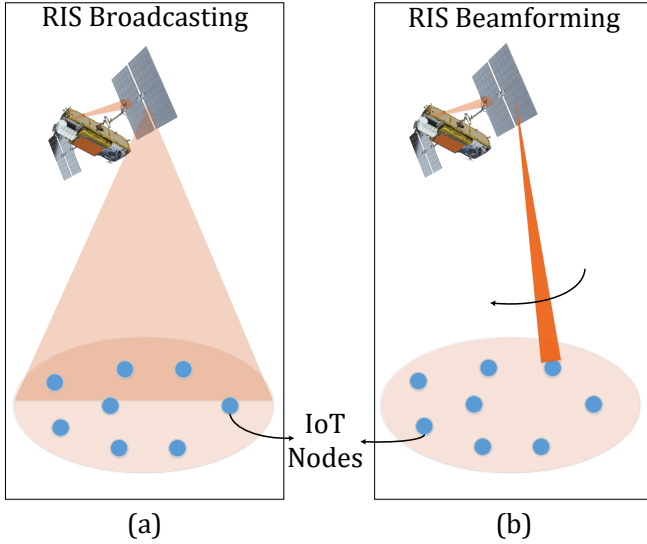


Fig. 2. RIS-assisted satellites can serve in two modes which are (a) RIS broadcasting and (b) RIS beamforming. In broadcasting case RIS acts as a scatterer for the incident wave while RIS performs specular reflection in beamforming schemes.

### B. Path Loss Models for RIS-assisted Communications

In this subsection, we describe the path loss models for RIS-assisted wireless communications in broadcasting and beamforming cases.

First, we consider the broadcasting case as illustrated in Fig. 2(a). If the transmitter is in the near field of RIS and the surface is at least ten times electrically larger than the wavelength,  $\lambda$ , the surface scatters the incident spherical wave. Scattering incident wave creates a large beam, which can cover multiple ground stations at the same time. As the transmitter antenna is relatively near the RIS unit deployed on the satellite, the scattering paradigm should be considered in the case of employing electrically large surfaces. The path loss model for RIS-assisted wireless communications in the case of broadcasting is modeled as follows [10]:

$$PL_{BC} \approx \frac{(4\pi)^\alpha (d_{tx} + d_{rx})^\alpha}{G_t G_r \lambda^\alpha A^\alpha}, \quad (3)$$

where  $d_{tx}$  and  $d_{rx}$  are the distances from transmitter antenna to RIS and the from RIS to receiver antenna, respectively. As  $d_{rx} \gg d_{tx}$ , the distance between transmitter antenna and RIS can be omitted and  $d_{rx} = d$ . Then, the expression can be written as:

$$PL_{BC} \approx \frac{(4\pi d)^\alpha}{G_t G_r \lambda^\alpha A^\alpha}. \quad (4)$$

$G_t$  and  $G_r$  denote antenna gain for transmitter and receiver antennas, respectively.  $A$  is the amplitude of the reflection coefficient of meta-atoms. It should be noted that the free-space path loss for RIS broadcasting scheme is not dependent to the number of RIS elements as seen in (4). In this scheme, RIS scatters the incident wave. Thus, while a wider coverage is obtained, the amount of energy per area is slightly lower.

On the other hand, the transmitted wave can be focused on the receiver in order to improve the received signal quality as

depicted in Fig. 2(b). Both the transmitter and receiver can be in the far-field of the RIS, or one of them can be found in the near-field of the RIS. The latter is the more appropriate model for satellite IoT systems, which includes onboard transmitter in satellites. Therefore, we utilize the near-field beamforming scheme for RIS. In other ways, it can be said that RIS operates as a specular reflection [16]. The path loss model for near-field beamforming scheme in RIS-assisted satellite is given as follows [10]:

$$PL_{BF} = \frac{64\pi^3}{G_t G_r d_x d_y \lambda^\alpha A^\alpha \left| \sum_{n=1}^N \frac{\sqrt{F_n^{\text{combine}}}}{d_{tx} d_{rx}} \right|^\alpha}, \quad (5)$$

where  $N$  is the number of meta-atoms.  $d_x$  and  $d_y$  are the size of each unit cell along the x-axis and y-axis, respectively.  $F_n^{\text{combine}}$  denotes the accounted normalized power radiation pattern on the received signal power and it is described as:

$$F_n^{\text{combine}} = F^{tx}(\theta_n^{tx}, \beta_n^{tx}) F(\theta_n^t, \beta_n^t) F(\theta_n^r, \beta_n^r) F^{rx}(\theta_n^{rx}, \beta_n^{rx}), \quad (6)$$

where  $F(\theta_n, \beta_n)$  shows the normalized radiation pattern for the elevation angle  $\theta_n$  and the azimuth angle  $\beta_n$  between RIS and transmitter antenna (or receiver antenna). The normalized radiation pattern for the elevation angle  $\theta$  and azimuth angle  $\beta$  is defined as follows [17]:

$$F(\theta, \beta) = \begin{cases} \cos^3(\theta), & \theta \in \left[0, \frac{\pi}{2}\right], \beta \in [0, 2\pi] \\ 0, & \theta \in \left(\frac{\pi}{2}, \pi\right], \beta \in [0, 2\pi] \end{cases} \quad (7)$$

It is worth to noting that in order to maximize the received power, the transmitter antenna has to be deployed to satellite such that its normal line is orthogonal to the surface. Namely,  $\theta_n^{tx} = \theta_n^t = 0$  for all unit cells. Without loss of generality, it is assumed that  $\theta_n^{rx} = \theta_n^r = \frac{\pi}{2} - \varphi$  and  $d_{rx} \gg d_{tx}$ . The most important issue in the RIS beamforming scheme is that the loss gradually decreases with the increasing number of elements.

### C. Rain Attenuation

Rain attenuation is one of major propagation impairment for satellite systems. Rain can cause scattering and absorption of the wave propagating through the atmosphere. The rain attenuation is described by ITU-R P.618-13 as [18]:

$$PL_{\text{rain}} = \xi_R L_E \text{ (dB)}, \quad (8)$$

where  $\xi_R$  and  $L_E$  are frequency-dependent specific attenuation coefficient described by ITU-R P.838 [19] and the effective path length. Firstly, we introduce the steps to find the value of  $\xi_R$ .

$$\xi_R = k (R_{0.01})^\nu \text{ (dB/km)}, \quad (9)$$

where  $R_{0.01}$  is the rainfall rate and can be obtained from ITU-R P.837 [20] for the location of a ground station.  $k$  and  $\nu$  denote the frequency-dependent coefficients given in ITU-R P.838 [19] as follows:

$$\begin{aligned} k &= [k_H + k_V + (k_H - k_V) \cos^2(\varphi) \cos(2\tau)] / 2 \\ \nu &= [k_H \nu_H + k_V \nu_V + (k_H \nu_H - k_V \nu_V) \cos^2(\varphi) \cos(2\tau)] / 2k, \end{aligned} \quad (10)$$

where  $\tau = \frac{\pi}{4}$  for circular polarization and all coefficients are listed in Table I for 4.25 GHz and 10.5 GHz.

In order to find the effective path length  $L_E$ , which is

$$L_E = L_R v_{0.01} \quad (\text{km}), \quad (11)$$

where  $v_{0.01}$  is the vertical adjustment factor modeled as follows:

$$v_{0.01} = \frac{1}{1 + \sqrt{\sin(\varphi) \left( 31 \left( 1 - e^{-(\varphi/(1+\chi))} \right) \frac{\sqrt{L_R \xi_R}}{f^2} - 0.45 \right)}}. \quad (12)$$

$f$  is the frequency in GHz and  $\chi$  is defined as [21]:

$$\chi = \begin{cases} 36 - |\text{latitude}|, & |\text{latitude}| < 36^\circ \\ 0, & \text{otherwise.} \end{cases} \quad (13)$$

Also,  $L_R$  is described as:

$$L_R = \begin{cases} \frac{L_G r_{0.01}}{\cos(\varphi)}, & \tan^{-1} \left( \frac{h_R - h_S}{L_G r_{0.01}} \right) > \varphi \\ \frac{(h_R - h_S)}{\sin(\varphi)}, & \text{otherwise.} \end{cases} \quad (14)$$

where  $h_S$  is the altitude of the ground station in km. Also,  $L_G$  is defined as:

$$L_G = \begin{cases} L_S \cos(\varphi), & h_R - h_S > 0 \\ 0, & h_R - h_S \leq 0 \end{cases} \quad (15)$$

where  $L_S$  is slant-path length calculated as follows:

$$L_S = \begin{cases} \frac{2(h_R - h_S)}{\sqrt{\sin^2(\varphi) + \frac{2(h_R - h_S)}{r_e} + \sin(\varphi)}}, & \varphi \leq 5^\circ \\ \frac{h_R - h_S}{\sin(\varphi)}, & \varphi > 5^\circ \end{cases} \quad (16)$$

where  $h_R$  is the effective height of the rain which is described by ITU-R P.839 [22] as:

$$h_R = h_0 + 0.36 \quad (\text{km}), \quad (17)$$

where  $h_0$  is the mean  $0^\circ$  isotherm height above mean sea level and it is site-specific value.

### III. LEO SATELLITES-ENABLED IOT NETWORKS

In this section, we describe the system model for RIS-assisted satellite communications with a transmitter antenna<sup>1</sup> in the near-field of RIS deployed on satellite. In order to maximize the received power, the transmitter antenna is required to be aligned with the normal line of the surface, which makes the angle between the normal line and antenna beam zero. Thus, the normalized radiation pattern takes maximum value as observed in (7). Furthermore, the distance  $d_{tx}$  between transmit antenna and the surface is very short compared to the distance to ground station. Hence, the wireless channel between transmitter and RIS can be omitted through the analysis. The received signal  $y$  can be introduced as

$$y = \sqrt{\frac{P_t}{PL}} \mathbf{g}^T \Phi \mathbf{h} x + w, \quad (18)$$

where  $x$  and  $w$  stand for the transmitted signal with power  $P_t$  and additive white Gaussian noise (AWGN) at receiver, respectively. The noise term,  $w$ , can be assumed to be distributed with  $\mathcal{CN}(0, N_0)$ .  $\mathbf{h}$  is the channel coefficient vector for the

<sup>1</sup>It should be noted that it is a receiver antenna for uplink communications.

TABLE I  
THE FREQUENCY-DEPENDENT COEFFICIENTS WHICH USED IN RAIN  
ATTENUATION CALCULATION FOR CIRCULAR POLARIZATION  
(ITU-R REC. P.838).

Coefficients	4.25 GHz	10.5 GHz
$k_H$	7.3420e-4	1.1926e-2
$k_V$	6.8259e-4	1.0526e-2
$\nu_H$	1.1489	1.2602
$\nu_V$	1.1034	1.2469
Polarization	Circular	Circular
$k$	7.084e-4	1.123e-2
$\nu$	1.127	1.254

link between RIS and receiver such that  $\mathbf{h} = [h_1, h_2, \dots, h_N]$ . On the other hand,  $\mathbf{g}$  stands for the channel coefficient for the link between transmitter and RIS. As transmit antenna is close to RIS, we can ignore the channel effects in between transmitter and RIS. Therefore,  $\mathbf{g}$  can be selected as the vector of all ones such that  $\mathbf{g} = \mathbf{1}_N$ . In this study, it is assumed that channel coefficients follow Rician distribution with the shape parameter of  $K = 10$ .  $\Phi$  denotes the RIS element responses and it can be shown as

$$\Phi = \text{diag} \{ A_1 e^{j\phi_1}, \dots, A_N e^{j\phi_N} \}, \quad (19)$$

where  $A_i$  and  $\phi_i$  are the amplitude and phase response of  $i$ -th RIS element. Throughout this study, RIS is assumed as a lossless device; therefore,  $A_i = A = 1, \forall i$ .

Next, regarding the received signal, the instantaneous SNR  $\gamma$  can be given as:

$$\gamma = \frac{|\mathbf{g}^T \Phi \mathbf{h}|^2 P_t}{N_0 PL}, \quad (20)$$

where  $PL$  is the total loss including free-space path loss<sup>2</sup> and rain attenuation. For free-space path loss calculation, (1) is utilized for satellite communications without RIS. In RIS-assisted case, there two different modes, which are related to the dimension of the RIS element unit. For RIS-assisted broadcasting scheme, (4) gives the free-space path loss, while (5) is the free-space path loss expression for RIS-assisted beamforming. Considering the SNR, the achievable data rate can be expressed as

$$R = \log_2(1 + \gamma) \quad (\text{bits/s/Hz}). \quad (21)$$

### IV. NUMERICAL RESULTS AND DISCUSSIONS

In this section, we evaluate comprehensive simulation and discuss simulation results. Firstly, we focus on downlink capacity for satellite IoT systems. Then, we investigate uplink capacity of satellite-supported IoT communications. We consider the simulation results for the two prominent bands for satellite IoT systems, namely C- and X-band. In simulations, the path loss model given in (1) is used for the case without RIS, while the models given with (4) for RIS broadcasting and (5) are used for RIS beamforming.

<sup>2</sup>It can be either RIS-assisted wireless communications or not. For RIS-assisted communications,  $PL_{BC}$  and  $PL_{BF}$  are employed for RIS broadcast case and RIS beamforming case, respectively. On the other hand, it is equal to  $PL_{FS}$  in case of wireless communications without RIS.

TABLE II  
THE LOCATION-SPECIFIC COEFFICIENTS WHICH USED IN RAIN  
ATTENUATION CALCULATION FOR CIRCULAR POLARIZATION  
(ITU-R REC. P.838 & ITU-R REC. P.839).

Parameters	Values
Location	Istanbul, Turkey
Latitude	41°N
Longitude	29°E
$h_0$	2.53 km
$R_{0.01}$	31.119
$h_S$	1 m
$h_{sat}$	800 km
$r_e$	6371 km

As the rain attenuation seriously changes with respect to the operating frequency, it is important to properly acquire the frequency-dependent coefficients such as  $k$  and  $\nu$ . For example,  $k$  is found for C- and X-band as  $7.084e-4$  and  $1.123e-2$ , respectively. Besides,  $\nu$  is equal to 1.127 and 1.254 for C- and X-band, respectively. It is worth to saying that these values are valid for circular polarization, i.e.  $\tau = \frac{\pi}{4}$ . All frequency-dependent coefficients are given in Table I.

Also, in simulations, we assume that the ground stations, i.e. IoT devices, are located in Istanbul, Turkey, which is located at 41° North latitude and 29° East longitude. Site-specific coefficients such as the mean 0° isotherm height above mean sea level  $h_0$  and the rainfall rate  $R_{0.01}$  is found as 2.53 km and 31.119 for Istanbul, Turkey. These parameters are summarized in Table II. As we investigate the LEO satellites, the satellite altitude  $h_{sat}$  is chosen as 800 km.

Another crucial point is that the characteristics of transmitter and receiver antennas as well as RIS characteristics. We evaluate the simulations by employing the antennas and RIS given in [10]. These antennas have the normalized radiation pattern  $F(\theta, \beta)$  defined as<sup>3</sup>

$$F^{tx}(\theta, \beta) = \begin{cases} \cos^{13}(\theta), & f = 4.25 \text{ GHz (C-band)} \\ \cos^{62}(\theta), & f = 10.5 \text{ GHz (X-band)}. \end{cases} \quad (22)$$

Furthermore, antenna gains are given as 14.5 dB and 21 dB for C-band and X-band antennas, respectively. As aforementioned above, the distance between transmit antenna and the surface is small. Hence,  $d_{tx}$  is selected as 1 m to keep near-field condition for both bands.  $d_{rx}$  is equal to the distance given by (2). In addition, some parameters of RISs are determined as follows: It is reported that RIS elements are designed in squares and their edge lengths are 0.012 m and 0.01 m for 4.25 GHz and 10.5 GHz, respectively.

The path loss exponent  $\alpha$  is chosen as 2, which is a generally accepted value. Additionally, the small-scale fading for the channel between RIS and receiver is modeled by Rice distribution with the shape parameter of  $K = 10$  in order to allow few non-line-of-sight (NLOS) paths. Last, the effective noise power for the overall system is chosen as  $-100$  dB. Table III summarizes the parameters which are employed in the calculation process of free-space path loss.

<sup>3</sup>Here, the normalized radiation pattern is given for only transmit antenna. It should be noted that this expression can also be utilized for receive antenna.

TABLE III  
THE PARAMETERS FOR FREE-SPACE PATH LOSS CALCULATION FOR RISs  
AND ANTENNAS OPERATING AT C-BAND AND X-BAND.

Parameters	4.25 GHz	10.5 GHz
$d_{tx}$	1 m	1 m
$d_{rx}$	$d$	$d$
$\alpha$	2	2
$d_x$ [10]	0.012 m	0.01 m
$d_y$ [10]	0.012 m	0.01 m
$G_t$ [10]	14.5 dB	21 dB
$G_r$ [10]	14.5 dB	21 dB
$F^{tx}(\theta, \beta)$ [10]	$\cos^{13}(\theta)$	$\cos^{62}(\theta)$
$F^{rx}(\theta, \beta)$ [10]	$\cos^{13}(\theta)$	$\cos^{62}(\theta)$
$\theta^t$	0	0
$\theta^r$	0	0
$\theta^{rx}$	$\frac{\pi}{2} - \varphi$	$\frac{\pi}{2} - \varphi$
$\theta^r$	$\frac{\pi}{2} - \varphi$	$\frac{\pi}{2} - \varphi$
$K$	10	10
$N_0$	$-100$ dB	$-100$ dB

### A. Downlink Performance Analysis

In this section, we investigate the downlink performance of satellite IoT networks in terms of achievable data rate in three cases: Without RIS, RIS broadcasting, and RIS beamforming. First, we compare the achievable data rate for conventional satellite systems with RIS-assisted satellites in Fig. 3(a) for C-band. The simulation results show that RIS-assisted satellites provide much higher capacity than conventional satellites, regardless of which scheme they operate. In fact, the RIS broadcasting scheme can provide up to  $10^4$  times higher achievable rate than the non-RIS case, while RIS beamforming can provide up to  $10^5$  times higher rate. In other words, the desired capacity can be obtained with a lower transmit power by using RIS structures in satellites. Next, we investigate the impact of the number of RIS elements in Fig. 3(b).

As the number of RIS elements increases, the achievable capacity for the RIS beamforming case increases, as expected. However, as given in (4), in the case of RIS broadcasting, the number of elements does not affect the performance. Due to specular reflection, RIS beamforming even with a single element can achieve more data rate than the broadcasting case. The main reason behind that is the scattering of energy in a wide area. It can be said that the broadcasting scheme can support more IoTs than the beamforming scheme because of a larger coverage area provided by the broadcasting. Last, as rain attenuation coefficients and the normalized radiation pattern are seriously dependent on the operating frequency the same analysis in C-band is evaluated for X-band in order to observe impacts. The simulation results are depicted in Fig. 3(c). For large  $N$  values, the achievable rate decreases to less than half, while the ratio of performance loss increases as the number of elements decreases. For example, in the case of a single element, the achievable rate decreases to almost one-fourth of that in the C-band.

Since LEO satellites are mobile with respect to the earth, the distance between them and the ground stations varies depending on the elevation angle. Distance is one of the major contributors to free space path loss. Therefore, we have performed the simulations by considering varying elevation

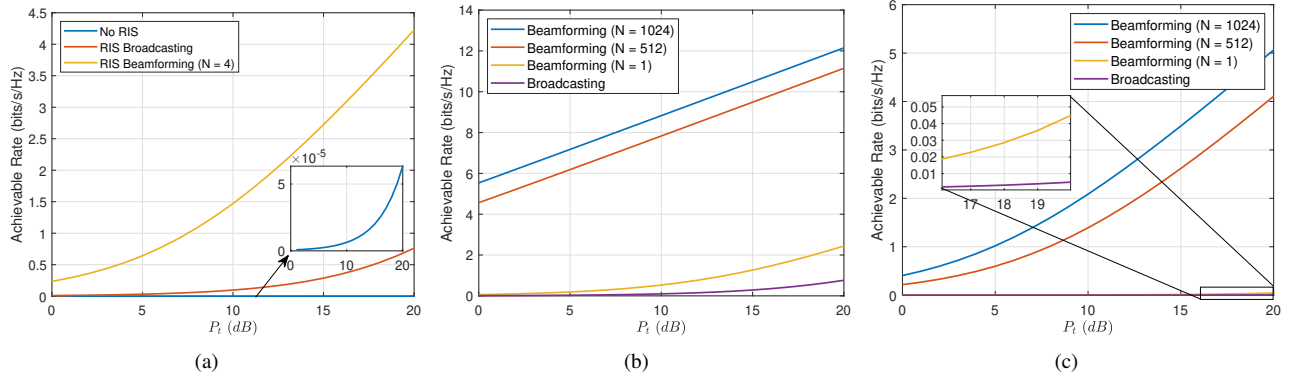


Fig. 3. Downlink achievable rate versus transmit power  $P_t$  for (a) comparison between non-RIS case and RIS-assisted satellites, (b) the various number of RIS elements in C-band, and (c) the various number of RIS elements in X-band. It should be noted that the elevation angle is  $\frac{\pi}{2}$ .

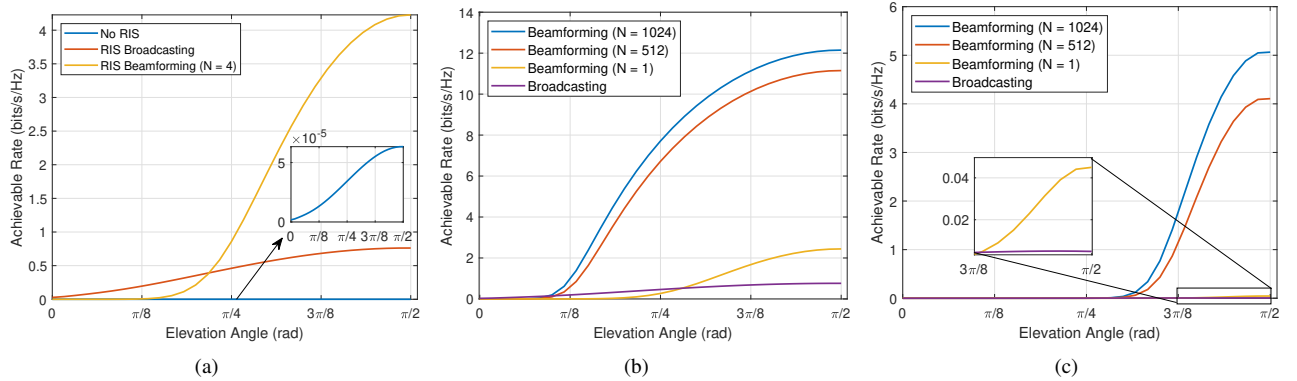


Fig. 4. Downlink achievable rate versus elevation angle  $\varphi$  for (a) comparison between non-RIS case and RIS-assisted satellites, (b) the various number of RIS elements in C-band, and (c) the various number of RIS elements in X-band. It should be noted that the transmit power is 100 W.

angles between zero and  $\frac{\pi}{2}$  rad. Fig. 4 denotes that the RIS beamforming overperforms than broadcasting and non-RIS cases. Since  $\theta^{rx}$  and  $\theta^r$  are defined as  $\theta^{rx} = \theta^r = \frac{\pi}{2} - \varphi$ , the elevation angle change the normalized received radiation pattern. Therefore, for the lower number of RIS elements at lower elevation angles, the RIS broadcasting scheme provides slightly better achievable rate than RIS beamforming. However, increasing the number of RIS elements compensates for the path loss increasing owing to the increased distance and decreased received radiation pattern as seen in Fig. 4(b) and Fig. 4(c).

### B. Uplink Performance Analysis

In this section, we analyze the uplink capacity of satellite IoT networks in three cases which are without RIS, broadcasting RIS, and beamforming RIS. Similar to downlink analyses above, we firstly investigate the advantage of utilizing RIS in satellites for IoT networks. Fig. 5(a) shows that RIS beamforming can provide up to  $10^5$  times higher uplink rate than non-RIS case. This result indicates that the battery and lifetime of battery-limited IoTs can be significantly increased with RIS-assisted satellites. Moreover, Fig. 5(b) shows that it is possible to obtain 3 dB more gain from transmit power by doubling the number of RIS elements (from 512 to 1024) for the same achievable data rate value. It is seen in Fig. 5(c) that the uplink data rate decreases significantly if the operating frequency is increased. As the number of RIS elements increases, the

rate of decrease in the achievable rate due to the increase in frequency degrades. Although increasing in the operating frequency reduces the achievable data rate performance, the higher frequency can be employed for small IoTs which cannot accommodate larger antennas. Fig. 6(a) shows that the RIS-beamforming scheme can serve with higher performance over a wider range of elevation angles than RIS broadcasting and non-RIS satellites. As seen in Fig. 6(b), increasing the number of RIS elements marginally improves the operation range in terms of elevation angle. Higher frequency limits the communications in a narrow elevation angle range as depicted in Fig. 5(c), which means that the communication duration in one period of a satellite is very short. It may cause many handovers between satellites in a short while.

Since the computational capacities and batteries of IoTs are small, it is possible to say that there are two main factors in extending battery life. These two basic factors are the operation of computationally complex processes such as transmission power and equalization. RIS-assisted satellite systems have two-fold advantages for IoT networks. First, RISs can provide the desired capacity at lower transmission power. The second is that it enables complex operations to be performed in an external environment (i.e. propagation medium) rather than on the device, thanks to the use of RIS units.



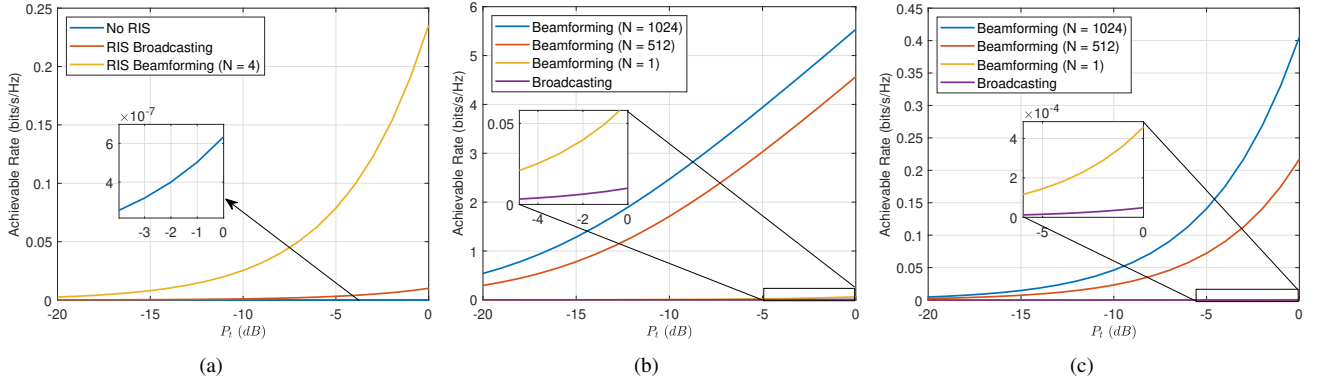


Fig. 5. Uplink achievable rate versus transmit power  $P_t$  for (a) comparison between non-RIS case and RIS-assisted satellites, (b) the various number of RIS elements in C-band, and (c) the various number of RIS elements in X-band. It should be noted that the elevation angle is  $\frac{\pi}{2}$ .

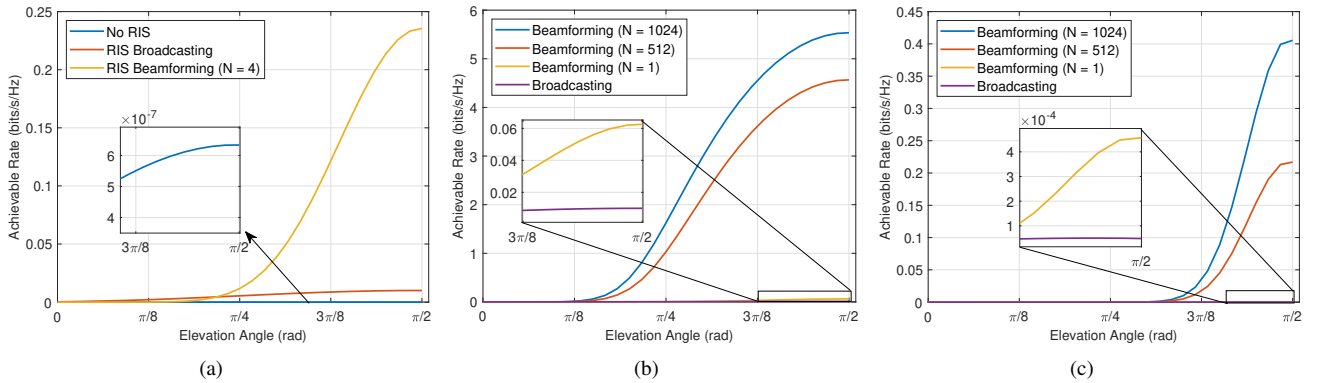


Fig. 6. Uplink achievable rate versus elevation angle  $\varphi$  for (a) comparison between non-RIS case and RIS-assisted satellites, (b) the various number of RIS elements in C-band, and (c) the various number of RIS elements in X-band. It should be noted that the transmit power is 1 W.

## V. OPEN ISSUES AND RESEARCH DIRECTIONS

Even though there are numerous open issues for RIS-assisted wireless communications, we discuss three of the most crucial issues for RIS-assisted satellites for IoT networks, which are the channel estimation, RIS deployment on satellites, and simultaneous wireless information and power transfer (SWIPT), with a focus on physical layer.

### A. Channel Estimation

Since RISs can change the amplitude and/or phase of the incident electromagnetic wave, they can largely eliminate the randomness of the propagation medium. However, it certainly needs high-quality channel state knowledge to obtain the maximum performance. Channel estimation thus plays a critical role in satellite communications for IoT networks to satisfy the desired QoS. Deep learning may be used for this purpose in order to achieve high efficiency under convincing channel conditions in channel estimation. Recently, for the channel estimation in RIS-assisted backhaul communications, we proposed a channel estimation framework based on graph attention networks (GATs) in [23]. By taking unseen nodes into consideration, the GAT can reduce computational complexity and improve learning performance. In the training process, the obtained signal samples and known pilot samples are assigned to the nodes and vertices of graphs, respectively. Since IoT devices lack the hardware infrastructure required for

training and using the deep learning model, it is reasonable to deploy the proposed GAT model to LEO satellites rather than IoT devices. By utilizing channel reciprocity, the channel coefficients can be obtained through the uplink pilot signaling. Without the need for downlink pilot signaling, phase adjustment can be performed by RIS by utilizing the coefficients found for the uplink channel. However, it is worth noting that this channel estimation cannot be employed in frequency division duplex communications for uplink and downlink. On the other hand, when using time division duplex, the signal processing can be performed through the propagation environment and RIS rather than IoTs, thus, it extends battery life.

### B. RIS Fabrication and Deployment

In the design of RISs, the environmental conditions must be considered. RISs that can be resilient to temperature variations between day and night should be developed. Although space may be assumed as a vacuum, it should be noticed that the entire space is filled with plasma and particles emitted from the Sun. The electronic elements of the communication unit may be affected by charged particles encountered by spacecraft in the Van Allen Belts. As a result, it is crucial to consider radiation-resistant RIS and any instrumentation that allows RIS operational.

How to implement the RISs into the LEO satellites is undeniably the most fundamental and first-glance question. Taking

into account the mechanical systems of satellites, it is obvious that it is necessary to address a significant design challenge. Especially, depending on the variations in their locations and elevation angles, the device itself is likely to shadow any or all of the meta-atoms. Based on the development of their structures, the authors envisage that conformal metasurfaces can be used in the coating of objects with irregular surfaces and arbitrary shapes. It is worth to remember that satellite systems have already utilized reflectarray antennas to reflect the incident beam with a constant phase [24]. These reflectarrays can be replaced by RISs to make satellites smart. As a result, satellites can reflect or scatter the incident wave with various phase configuration. Interdisciplinary studies can make novel RIS designs possible. For example, it may be possible to place many RIS elements in a wide area by covering the lower faces of the satellite solar panels with RIS. Moreover, the antenna subsystems currently on satellites might be replaced by RISs.

### C. Simultaneous Wireless Information and Power Transfer

As IoT nodes are power-limited devices, energy harvesting can be considered in SWIPT framework. RIS-aided SWIPT has been proposed to achieve significant performance gain in energy harvesting [25]. SWIPT can be a solution to keep power-constrained IoT systems running for a long time. But, its applications in satellite-IoT systems are lacking in the literature. Considering the power transfer capacity of space solar satellites with microwave waves [26], the joint utilization of RISs and rectenna arrays can further improve the energy-efficiency of IoT networks. To shortly and precisely emphasize, RIS-assisted satellites for SWIPT in IoT networks deserve more attention in the future.

## VI. CONCLUDING REMARKS

Ubiquitous connectivity and user-centric communications are the strict requirements of 6G networks. As the number of the connected devices and Internet of Things (IoTs) networks are expected to increase exponentially, LEO satellite networks gain attention to serve as the backhaul/fronthaul connectivity solution to densely deployed IoT sensors. However, the current systems under consideration either have a very high path loss or require steerable antennas in IoT devices. Considering these drawbacks of the previously proposed system models, we introduce an overview of the RIS-assisted LEO satellite framework for energy-efficient IoT networks in this study. The motivation behind the RIS communications in satellite-IoT are given using extensive numerical results throughout the study. The potential gain in terms of the transmission powers of lightweight IoT nodes are quantified. Furthermore, open issues regarding the proposed system model are also discussed.

## REFERENCES

- [1] Huawei, "Touching an intelligent world," <https://bit.ly/38KHmT>, 2019, (Accessed on 01/07/2021).
- [2] McKinsey Global Institute, "The Internet of Things: Mapping the value beyond the hype," <https://mck.co/3igecTk>, June 2015, (Accessed on 01/08/2021).
- [3] Deloitte, "The Internet of Things: a technical primer," <https://bit.ly/35HPPc8>, 2018, (Accessed on 01/08/2021).

- [4] S. Kota and G. Giambene, "Satellite 5G: IoT use case for rural areas applications," in *International Conference on Advances in Satellite and Space Communications*, 2019, pp. 24–28.
- [5] C. A. Hofmann and A. Knopp, "Direct access to GEO satellites: An Internet of Remote Things technology," in *IEEE 5G World Forum*, 2019, pp. 578–583.
- [6] R. Barbau, V. Deslandes, G. Jakllari, J. Tronc, J.-F. Chouteau, and A.-L. Beylot, "NB-IoT over GEO satellite: performance analysis," in *Advanced Satellite Multimedia Systems Conference and the Signal Processing for Space Communications Workshop*, 2020, pp. 1–8.
- [7] Z. Qu, G. Zhang, H. Cao, and J. Xie, "LEO satellite constellation for Internet of Things," *IEEE Access*, vol. 5, pp. 18 391–18 401, 2017.
- [8] S. Cluzel, L. Franck, J. Radzik, S. Cazalens, M. Dervin, C. Baudoin, and D. Dragomirescu, "3GPP NB-IoT coverage extension using LEO satellites," in *IEEE Vehicular Technology Conference*, 2018, pp. 1–5.
- [9] E. Basar, M. Di Renzo, J. De Rosny, M. Debbah, M.-S. Alouini, and R. Zhang, "Wireless communications through reconfigurable intelligent surfaces," *IEEE Access*, vol. 7, pp. 116 753–116 773, 2019.
- [10] W. Tang, M. Z. Chen, X. Chen, J. Y. Dai, Y. Han, M. Di Renzo, Y. Zeng, S. Jin, Q. Cheng, and T. J. Cui, "Wireless communications with reconfigurable intelligent surface: Path loss modeling and experimental measurement," *arXiv preprint arXiv:1911.05326*, 2019.
- [11] L. Dai, B. Wang, M. Wang, X. Yang, J. Tan, S. Bi, S. Xu, F. Yang, Z. Chen, M. Di Renzo *et al.*, "Reconfigurable intelligent surface-based wireless communications: Antenna design, prototyping, and experimental results," *IEEE Access*, vol. 8, pp. 45 913–45 923, 2020.
- [12] K. Tekbilyk, G. K. Kurt, A. R. Ekti, and H. Yanikomeroglu, "Reconfigurable intelligent surfaces in action for non-terrestrial networks," *arXiv preprint arXiv:2012.00968*, 2020.
- [13] Q. Wu and R. Zhang, "Intelligent reflecting surface enhanced wireless network via joint active and passive beamforming," *IEEE Trans. on Wirel. Commun.*, vol. 18, no. 11, pp. 5394–5409, 2019.
- [14] 3GPP, "Study on Narrow-Band Internet of Things (NB-IoT)/enhanced Machine Type Communication (eMTC) support for Non-Terrestrial Networks (NTN)," 3rd Generation Partnership Project (3GPP), Technical Report 36.763, 01 2021, release 17. [Online]. Available: <https://portal.3gpp.org/desktopmodules/Specifications/SpecificationDetails.aspx?specificationId=3747>
- [15] C. Huang, A. Zappone, G. C. Alexandropoulos, M. Debbah, and C. Yuen, "Reconfigurable intelligent surfaces for energy efficiency in wireless communication," *IEEE Trans. on Wirel. Commun.*, vol. 18, no. 8, pp. 4157–4170, 2019.
- [16] S. W. Ellingson, "Path loss in reconfigurable intelligent surface-enabled channels," *arXiv preprint arXiv:1912.06759*, 2019.
- [17] C. A. Balanis, *Antenna Theory: Analysis and Design*. John Wiley & Sons, 2016.
- [18] ITU-R, "Propagation data and prediction methods required for the design of Earth-space telecommunication systems," International Telecommunication Union (ITU), Recommendation P.618-13, 12 2017. [Online]. Available: [https://www.itu.int/dms\\_pubrec/itu-r/rec/p/R-REC-P.618-13-201712-I!!PDF-E.pdf](https://www.itu.int/dms_pubrec/itu-r/rec/p/R-REC-P.618-13-201712-I!!PDF-E.pdf)
- [19] —, "Specific attenuation model for rain for use in prediction methods," International Telecommunication Union (ITU), Recommendation P.838-3, 03 2005. [Online]. Available: [https://www.itu.int/dms\\_pubrec/itu-r/rec/p/R-REC-P.838-3-200503-I!!PDF-E.pdf](https://www.itu.int/dms_pubrec/itu-r/rec/p/R-REC-P.838-3-200503-I!!PDF-E.pdf)
- [20] —, "Characteristics of precipitation for propagation modelling," International Telecommunication Union (ITU), Recommendation P.837-7, 06 2017. [Online]. Available: [https://www.itu.int/dms\\_pubrec/itu-r/rec/p/R-REC-P.837-7-201706-I!!PDF-E.pdf](https://www.itu.int/dms_pubrec/itu-r/rec/p/R-REC-P.837-7-201706-I!!PDF-E.pdf)
- [21] G. Maral, M. Bousquet, and Z. Sun, *Satellite communications systems: systems, techniques and technology*. John Wiley & Sons, 2020.
- [22] ITU-R, "Rain height model for prediction methods," International Telecommunication Union (ITU), Recommendation P.839-4, 09 2013. [Online]. Available: [https://www.itu.int/dms\\_pubrec/itu-r/rec/p/R-REC-P.839-4-201309-I!!PDF-E.pdf](https://www.itu.int/dms_pubrec/itu-r/rec/p/R-REC-P.839-4-201309-I!!PDF-E.pdf)
- [23] K. Tekbilyk, G. K. Kurt, C. Huang, A. R. Ekti, and H. Yanikomeroglu, "Channel estimation for full-duplex RIS-assisted HAPS backhauling with graph attention networks," *arXiv preprint arXiv:2010.12004*, 2020.
- [24] J. Huang, "Reflectarray antenna," *Encyclopedia of RF and Microwave Engineering*, 2005.
- [25] Q. Wu and R. Zhang, "Weighted sum power maximization for intelligent reflecting surface aided SWIPT," *IEEE Wireless Commun. Lett.*, vol. 9, no. 5, pp. 586–590, 2019.
- [26] C. A. M. Bergsrud, R. Bernaciak, S. Chaieb, and J. Casler, "Rectenna array equipped on satellites," *Journal of Spacecraft and Rockets*, vol. 53, no. 3, pp. 480–493, 2016.